Accepted Manuscript

Geodynamic implications of temporal gravity changes over Tibetan Plateau

Carla Braitenberg & C.K. Shum

To appear in: *Italian Journal of Geosciences*

Received date: 29 May 2015

Accepted date: 16 October 2015

doi: 10.3301/IJG.2015.38

Please cite this article as:

C. Braitenberg & C.K. Shum - Geodynamic implications of temporal gravity changes over Tibetan Plateau, *Italian Journal of Geosciences* 10.3301/IJG.2015.38

Geodynamic implications of temporal gravity changes over Tibetan Plateau

Carla Braitenberg[1] and C.K. Shum[2, 3]

1 Dept. of Mathematics and Geosciences, University of Trieste, Via Weiss 1, 34100 Trieste, Italy, email: berg@units.it

2 Division of Geodetic Science, School of Earth Sciences, Ohio State University, Columbus, Ohio 43210, USA,

3 Institute of Geodesy & Geophysics, Chinese Academy of Sciences, Wuhan 430077, China, email: ckshum@osu.edu

Abstract

The Tibetan Plateau is one of the most geologically dynamic systems and the highest plateau in the world with ongoing three-dimensional crustal deformation. The Plateau is uplifting and deforming horizontally as observed by present-day global navigation satellite system (GNSS) and repeated leveling measurements. Crustal mass is conservative and less dense than the mantle, thus the horizontal shortening must be accompanied by crustal thickening and horizontal extrusion. According to the level of isostatic compensation, the thickening is partitioned into topographic uplift and Moho deepening. Here, we investigate the mass change induced gravity signal observed at or near the crust, and discuss whether this signal could be detected using terrestrial or satellite gravity observations. We set up a model for the Tibetan Plateau crustal thickening and calculate the expected gravity signal. The predictions are then compared with the present-day gravity changes observed by GRACE and with published *in situ* absolute gravity rates. We conclude that the crustal thickening signal cannot be neglected and that it contributes significantly to the observed signal. Those studies with focus on the mountain glacier and hydrologic mass fluxes should be aware that, if neglected, the crustal signal could introduce a significant bias. The observations give a positive gravity rate over central Tibetan Plateau, unexplained by the hydrologic or cryospheric signals, and a negative rate over the Himalayas and at its foothill, which is attributable to terrestrial hydrologic signals including human depletion of

groundwater. Our model shows that the positive gravity rate could be explained by elevation uplift, and a stable or upwelling Moho. The negative gravity change signal is due primarily to the strong elevation-gradient at the foothill of the Himalayas, and to an uplift accompanied by crustal thickening and Moho lowering. The estimated gravity rates can be used when defining the requirements on future gravity missions, as the tectonic signal should be resolved in order to improve its separation from hydrologic and/or cryospheric processes.

Introduction

The Tibetan Plateau is an active geodynamic system, which has been continuously deforming driven by the northwards subduction of the Indian plate and the relatively stable and rigid platforms of Eurasia forming a non-deformable lithospheric barrier surrounding the Plateau. The Yarlung Zangbo line represents the suture between the India and Eurasian plates (Figure 1). The active deformation front migrated southwards from this suture at the onset of collision to the Main Boundary Thrust, where the Lesser Himalaya sequences are thrusted over the Quaternary molasses of the India plate (DE CELLES *et alii*, 2002). The subduction of the Indian plate has been demonstrated by regional seismic studies, which have illuminated the gently dipping Indian lithosphere subducting below the Himalayas and reaching at least as far as the Tibetan Yarlung Zangbo suture (e.g. PRIESTLEY *et alii.*, 2008; LI *et alii* 2008).

The subduction of India reduces the volume space for the Plateau, which dynamically responds through deformation. The deformation is inhomogeneous as revealed by the *in situ* surface velocities derived from continuous and episodic GPS observations (WANG *et alii*, 2001; LIANG *et alii*, 2013; GAN *et alii*, 2007). The horizontal velocities respect to a reference system anchored to northern Asia and Europe are near to NS in the central Plateau and turn east at the eastern plate margin, with high curvature iso-amplitudes bending around the eastern syntaxis. Analogous bending is found around the western

syntaxis, although not as pronounced. The velocities degrade northwards, being highest in the Indian Plate. The northwards decreasing velocities imply that the Plateau is not moving northward as a rigid block, but that it is contracting in NS direction, the velocity at the northern border being very low. Vertical velocities from GPS are less accurate but nonetheless revealed significant information showing that the Plateau is presently uplifting. The uplift and the contraction are to be considered two aspects of the same phenomenon, which is the ongoing northward crustal shortening and eastward extrusion accompanied by thickening. When crust thickens, the vertical expansion is partitioned in topographic uplift and Moho sinking. Both effects change the mass along the lithospheric columns: uplift adds mass to the surface, replacing air with rock; the lowering of the Moho replaces the denser mantle with less dense crust. Mass changes can be deduced from observations of the gravity field, either terrestrial or from satellites, such as the Gravity Recovery And Climate Experiment or GRACE mission (TAPLEY *et alii* 2004). The gravity signal is opposite in the two cases, being a negative and positive gravity rate for Moho lowering and topographic uplift, respectively. We could imagine the uplift of topography is due to an upward dynamic push from below without crustal thickening, which would imply an upwelling of the Moho and replacement of crust with the denser mantle. In this case a mass increase at the Moho is obtained, the surface level would arise, with a positive gravity change. Figure 2 illustrates this concept in a schematic. The geodynamic gravity change competes with mass changes due to the hydrologic and cryospheric processes (ERKAN *et alii*, 2011). Independent from the focus of study, whether it is climatic, hydrologic or geodynamic, it is important to be able to separate these signals. Gravity measurements have been traditionally terrestrial, either with the difficult to transport absolute gravimeter or with the more common relative gravimeter. Observations of the geodynamic signal require repeated gravity observations, for which the absolute gravimeter is ideal. The relative gravimeters, instead require stable stations to detect the time-varying gravity signal. This means that, in the study area, the station network should include stations both in the Plateau and in the China craton,

covering an enormous area hundreds of km wide and including huge changes in the gravity values due to the height difference between the stable craton and the high topography. The small gravity changes in time would be very difficult to detect due to the uncertainties in the instrumental drift correction when stations are distant. The absolute observations do not have this problem and repeated single point measurements can be made without requiring a reference network. The number of stations that can be occupied is very limited due to the facilities required to make the observations. Only since a few years absolute gravimeters have become more portable and can be efficiently used for field measurements. Satellite gravimetry to observe geodynamic signals at large scale has been possible since launch of the twin satellite mission GRACE (TAPLEY *et alii*, 2004). The GRACE mission was targeted to reveal gravity field changes in time and has acquired today already over 12 years of continuous global gravity field time series. The Gravity Field and Steady-State Ocean Circulation Explorer or GOCE mission (FLOBERGHAGEN *et alii*, 2011) has superior resolution allowing geologic structures to be distinguished (BRAITENBERG, 2014; 2015), but had a too short of a mission life span (2009–2013) to potentially allow the detection of climatic or geodynamic changes. In the present paper we first make a review on the time variable gravity observations over the Tibetan Plateau, both from absolute gravity observations and from GRACE. We then estimate the expected signal for the varying gravity change based on the vertical uplift and assuming different models for Moho depth variations, and compare the predictions with the published observed rates.

Observations of gravity time variations

Absolute gravity measurements

The first observations of gravity change in the Tibetan Plateau were made with repeated absolute gravity measurements in three stations of the Chinese National Geodetic Observation Network, Lhasa (29.66°N, 91.10°E, 3643 m a.s.l) on the Plateau, and Kunming (25.15°N, 102.76°E, 1952 m a.s.l) and

Dali (25.61°N, 100.25°E, 1958 m a.s.l) at the South Eastern foot of the Plateau (SUN *et alii*, 2009). Repeated measurements spanned the years 1990 to 2007, with the standard deviation of the absolute gravity measurements varying between 1 and 5 10^{-8} m/s^2 (μGal = 10^{-8} m/s^2) according to instrument type and repetition number of the observations. Between 1990 and 1995 the JILAG-3 and JILAG-5, from 1996 the FG5-112, FG5-107 and FG5-210 were used. The accuracy of the instrument is not given in the publication, but TIMMEN *et alii* (2006) estimate the accuracy of one FG5 instrument (FG5-220) to be ±3 10^{-8} m/s^2, while the JILAG-3 has been estimated by TORGE (1991) to have an accuracy of ±7 10^{-8} m/s^2 and an instrumental precision of ±4 10^{-8} m/s^2. The JILAG-3 was found to have a bias of +9 10^{-8} m/s^2 compared to two different FG5 instruments (101 and 220) by TIMMEN *et alii* (2008). Due to the bias the estimated negative gravity rate could be a bit overestimated in SUN *et alii* (2009). The Lhasa station had the highest gravity decrease of –1.97±0.66 10^{-8} m/s^2/yr, with station Kunming having the rate of –1.42±0.38 10^{-8} m/s^2/yr and Dali being relatively stable with a rate of –0.41±0.24 10^{-8} m/s^2/yr. Here and in the following, the uncertainty is given in terms of one standard deviation. The values have been summarized in Table 1. The gravity signal observed at the Dali station was thought to be affected by the annual water level change in a lake 100 m from the station. The data of the three stations were not corrected for the effects of loading from snow accumulation and melt, hydrology and the atmosphere. The vertical movement of the stations had been measured since 1990 by GPS belonging to networks established for tectonic studies (WANG *et alii*, 2001; GAN *et alii*, 2007). All three stations, Lhasa, Kunming and Dali exhibited positive vertical displacements, respectively +0.8±0.5, +2.3±0.5 and +0.5±0.5 mm/yr (SUN *et alii*, 2009). The gravity stations move upwards together with the Plateau, which causes two effects on the measured gravity with opposite sign. Gravity decreases with height at the standard rate of –0.31 10^{-8} m/s^2 /mm (TORGE, 2001) but the uplift generates a mass surplus due to the topographic mass increase, which is estimated as +0.11 10^{-8} m/s^2/mm for a density of 2700 kg/m^3. The latter effect is a first order estimate adopting the Bouguer

plate correction, valid for an infinite plate (e.g. HOFMANN-WELLENHOF & MORITZ (2006)). Using the Bouguer plate approximation and the approximated height gradient for a spherical earth, SUN *et alii* (2009) calculated the net effect of uplift for the terrestrial measurement as –0.19 10^{-8} m/s^2/mm. A further contribution was ascribed to the denudation of a total volume of 1.5 km^3/yr from the entire Tibet Plateau (METIVIER *et alii*, 1999, LAL *et alii*, 2004). Distributing this mass over the Plateau and calculating again the effect of a horizontal plate, it contributed to an estimated gravity change of –0.25 ±0.1 10^{-8} m/s^2/yr. The resulting height and denudation corrected gravity change rates in the stations of Lhasa, Kunming and Dali amounted to, respectively, –1.56±0.67, –0.73±0.39 and –0.06±0.26 10^{-8} m/s^2/yr (SUN *et alii*, 2009). These rates are the most accurate that can be obtained to date, as they are terrestrial observations made with highly sophisticated instrumentation. The final result consists of a negative gravity rate, which cannot be attributed to the uplift or the denudation. A further gravity source can be ascribed at crust-mantle level, where the greatest density jump occurs and therefore the most important crustal contribution to gravity. SUN *et alii* (2009) estimate this effect again in the approximation of a Bouguer infinite slab with density equal to the difference between the assumed crustal (2,600±100 kg/m^3) and mantle density (3,400±100 kg/m^3), which amounted to 800±140 kg/m^3. The gravity change related to this layer at Moho depth was estimated as 0.34 10^{-8} m/s^2/cm in the Bouguer plate assumption, which implied that an average observed negative rate of –0.78 10^{-8} m/s^2/yr could be due to a Moho lowering of 2.3 cm/yr. The chosen density contrast of 800±140 kg/m^3 across the mantle is quite high compared to other findings (e.g. BRAITENBERG *et alii.*, 2000b). WANG *et alii.*, (2007) further find that lower crustal and upper mantle densities change laterally across Tibet and that the density contrast across the Moho is lower than 500 kg/m^3. A 30% smaller density contrast (respect to 800 kg/m^3) would lead to an increased Moho lowering of 3.3 cm/yr.

Ratio between gravity change and topographic uplift

The parameter used to distinguish between crustal uplift and crustal thickening with Moho lowering is the ratio between gravity change rate and topographic uplift rate. The ratio is motivated by the first order estimates obtained applying the Bouguer plate assumption. Later in the paper we calculate the correct gravity effect using the discretization with prisms, but nonetheless here we discuss the relation between gravity and uplift using the approximation of the flat infinite plate (Bouguer plate), which allows to give a general insight to the problem. To first order the gravity effect of an infinite plate of density ρ and thickness h is $dg=2\,\pi\,\rho\,G\,h$, G being the gravitational constant G=6.67 10^{-11} N/(kg/m)^2. The effect of an increase Δh in topography of density ρ_c is then $\Delta g_1 = 2\,\pi\,\rho_c\,G\,\Delta h$. This corresponds to the mass change at the top of the topography in Figure 2a. The ratio between the gravity change and the topography change is $\Delta g_1/\Delta h = 2\,\pi\,\rho_c\,G$. If the topographic increase is due to a crustal uplift without crustal thickening, then we must add the mass increase at Moho level to the calculation. The mass change at Moho level is shown in Figure 2a in red. The gravity change due to the mass at Moho level will be $\Delta g_2 = 2\,\pi\,(\rho_m - \rho_c)\,G\,\Delta h$, and the net gravity change (topographic uplift and mass at Moho level) $\Delta g_3 = 2\,\pi\,\rho_m\,G\,\Delta h$. The ratio between gravity change and uplift will be $\Delta g_3/\Delta h = 2\,\pi\,\rho_m\,G$. The above computation is under the assumption that the terrestrial measurements have been corrected for the gravity change due to the increase in height.

If we include the uplift effect in the ratio, we obtain for the pure topographic height change the ratio $\Delta g_1/\Delta h = 2\,\pi\,\rho_c\,G - 0.310^{-8}$ m/s^2/mm and for the case with Moho uplift $\Delta g_3/\Delta h = 2\,\pi\,\rho_m\,G - 0.3\ 10^{-8}$ m/s^2/mm. With standard crust and mantle density values as tose used in the next chapter, ρ_c = 2,670 kg/m^3 and ρ_m = 3,200 kg/m^3, the change ratios are $\Delta g_1/\Delta h$ = 0.12–0.30 10^{-8} m/s^2/mm = –0.19 10^{-8} m/s^2/mm (pure topography uplift) and $\Delta g_3/\Delta h$ = 0.13–0.30 10^{-8} m/s^2/mm = –0.17 10^{-8} m/s^2/mm (topographic uplift and Moho uplift). The values have been summarized in Table 2. In studies

concerned with postglacial uplift the ratio is termed viscous ratio (e.g., Sato *et alii*, 2012) and associated to the mantle influx below the uplifting area.

At Lhasa station we divide the gravity rate by the uplift rate obtaining the observed ratio dg/dh=-1.97 10^{-8} m/s^2/yr/0.8 mm/yr = –2.4 10^{-8} m/s^2/mm, for Kunming it is dg/dh = –1.42 10^{-8} m/s^2/yr/2.3 mm/yr = –0.62 10^{-8} m/s^2/mm and for Dali it is dg/dh = –0.41 10^{-8} m/s^2/yr/0.5 mm/yr = 0.82 10^{-8} m/s^2/mm. The observed ratios show high variability with the Lhasa stations having a much greater value compared to the other two stations. The ratios are very large when compared to the expected values in the simple Bouguer assumption and show that a 3D calculation scheme is necessary in order to explain the observations. Another problem could be due to uncertainties in the estimated uplift rates, which could be underestimated due to insufficient length of time series or errors in calculated rates, or else the gravity rates could have been overestimated due to a possible bias using different absolute gravity measurements. Ratio values in South-East Alaska have been published by SATO *et alii*, (2012) where they are lower and near to –0.2±0.01 10^{-8} m/s^2/mm after correction of the mass effects of the present-day glacier mass loss, and reasonably agree with predictions from postglacial rebound models.

The terrestrial measurement has the drawback that it is a local measurement, and the common practice of extrapolation of the measurement over the entire Plateau in contemporary studies, would imply a homogeneous signal over the Plateau, which is an unrealistic assumption.

Satellite observations

The gravity rate observations from GRACE have a spatial resolution of about 330 km, which corresponds to an averaged rate over an area of about that size. The averaging is made in the data processing that uses a large amount of continuous along track observations on board the satellite. The resolution is given by the maximum degree 60 of the spherical harmonics expansion for the published monthly gravity changes. Significant changes have been published which reveal negative change rates

over the Plateau with variations in different areas of the Plateau. MATSUO & HEKI (2010) determine the gravity change from GRACE observations for 2003–2009 and attribute the yearly and long term gravity change to hydrologic effects concentrated at the outer border of the Tibetan Plateau, estimated to be 47±12 Gigaton/yr mass loss. These authors mentioned the uncertainty in the contribution of isostatic or tectonic uplift, but did not consider the effect of crustal thickening. The GRACE observations were filtered with a Gaussian filter of radius 400 km to reduce short wavelength noise. YI AND SUN (2014) extend the time series of GRACE to 2003–2012 and confirmed the spatially variable gravity change rate. They express the gravity signal in terms of equivalent surface mass loss in the Himalayas and in the Indian region south of the central Himalayas. Two sources are assumed to be responsible for the negative change rate, the mountain glacier melt (–35±5.8 Gtons/yr), and the Indian groundwater depletion (–30.6±5 Gtons/yr). The observations have been corrected for soil moisture effects predicted from the terrestrial storage model of the Global Land Data Assimilation System (GLDAS) Data Products (RODELL *et alii*, 2004). The result is a significant positive gravity residual over the entire central Tibetan Plateau in the order of 0.4–0.6 10^{-8} m/s^2/yr which cannot be explained by the terrestrial storage model. In the Himalayan foot hills the gravity residual results to be negative, which is interpreted as due to hydrologic depletion. The authors use a simple Bouguer plate model of a rising topography at a constant rate of 2 mm/yr to estimate the order of magnitude of the expected gravity change. The effect due to postglacial rebound is thought to be negligible. The authors find that further work must be done to explain the origin of the observed positive gravity change rate in central Tibetan Plateau.

Gravity variations through crustal thickening

In the previous paragraph we have shown that it is an open question whether crustal thickening in the Tibetan Plateau is observable by gravity, and that there is a lack of geodynamic modeling which goes

beyond the approximate Bouguer plate estimate. Here we make a more realistic approach with a complete forward calculation of the signal with different model situations taking into account topography change rates and Moho depth changes obeying different assumptions for the isostatic response mechanism.

The goal being to calculate the gravity variation, we must model the expected mass change rate at topography and Moho level. The mass contributions above sea level are placed at the surface of the topographic Plateau. The digital elevation model of ETOPO1 (AMANTE & EAKINS, 2009) is discretized into rectangular prisms and an average uplift rate is applied which determines the mass to be added at the top of the starting prism model. Density is set to 2,670 kg/m^3, the average value for granite (SCHÖN, 2011). Density acts as a linear scaling factor for gravity, therefore deviations from this value linearly modify the calculated gravity. The distribution of GPS stations over the Tibet Plateau is inhomogeneous, with no stations with available data located in western Tibetan Plateau. To not introduce a bias due to lack of data coverage, we apply a uniform uplift rate to the high Plateau, limiting the uplifting area to elevations greater than 4,000 m. The rationale of adopting this height value is motivated by observing the uplift rate profile published in Fig. 7 of LIANG *et alii* (2013), with rate values rapidly decreasing when the elevation is lower than 4,000 m. Physically it shows that only the high Plateau and the Himalayas are affected by the uplift, the lower surrounding areas being stable or subsiding. Repeated leveling has determined uplift rates in Eastern Tibetan Plateau over 40 years of observation, revealing the rates of 6±1 mm/yr (HAO *et alii*, 2014), when compared to the stations in the Sichuan basin which are sinking, lead to relative rates of 8±2 mm/yr. Compared to the GPS derived rates calculated over the shorter time interval of 10 years, the rates from leveling are systematically higher by a factor of two to six.

We use three models in our simulation of uplift, two end-member models and one mixed model. The first case assumes the uplift being due to an upwelling of the mantle, motivated by the requirement at

mantle level to give away space to the steady state subduction of the Indian plate. The crustal thickness does not change and Moho is uplifting by the same rate of the increasing topography (Figure 2A). We used the model in the previous chapter when estimating the ratio between gravity change and uplift in the Bouguer plate approximation. The mass change at Moho level is equal to the density difference between mantle and crust $\Delta\rho=(\rho_m - \rho_c)$ multiplied by the uplift topographic rate $\Delta h/dt$. A smaller positive gravity signal is obtained in a variant of the first model, with no mass change at Moho level, which corresponds to a lateral mass input into the Tibetan crust involving no mantle movement and mass change is only at the surface accompanying the observed topographic growing (not shown in Figure 2). The second case assumes that the uplift is due to crustal thickening, where the thickening rate is partitioned into a topographic uplift and a Moho lowering (Figure 2B). The isostatic equilibrium is assumed to be maintained. The Tibetan Moho has been shown previously (BRAITENBERG *et alii,* 2000a,b; 2003) using the methodology developed in BRAITENBERG *et alii* (2002) to obey the predictions of a flexure model subject to vertical topographic loading and horizontal compressional forces (SHIN *et alii* 2007; 2009; 2015). The large amplitude variations obey the lithospheric flexure involving longer wavelengths, and minor amplitude shorter wavelength oscillations obey folding due to horizontal compression. Here we limit calculations to the greater amplitude signal, the flexural part, which is in good agreement with the gravity observations from GOCE (SAMPIETRO *et alii*, 2014). Assuming a steady state process for the uplift, a time lag between uplift and flexural Moho response is irrelevant, as this would induce a visible time shift only in case of non-stationary uplift. The third model is a combination of the first and second model, with crustal thickening applied to the Himalayas and other orogens surrounding the Tibet plateau and Moho uplift to the remainder part of the Plateau (Figure 2C).

According to the model shown in Figure 2B, the net mass change is at the surface of the topographic relief and at the base of the Moho, with a mass increase above surface and a mass decrease at Moho

level in the case of isostatic compensation, with crust replacing mantle. The mass decrease at the Moho depends on the flexural parameter of rigidity. Rigidity zero is one end-member, which corresponds to the local compensation Airy model, with maximal Moho lowering and smallest topographic uplift for a given crustal thickening rate. High flexural rigidity, or equivalent lithospheric thickness, is the other end-member, where increasingly less Moho is lowered, and crustal thickening is entirely transferred to topographic uplift. Previous results have shown (BRAITENBERG *et alii*, 2003, SHIN *et alii*, 2007) that the elastic thickness is low over the Plateau, between 10 and 30 km, which implies that the flexural response to mass changes is close to local compensation. We use our software Lithoflex (http://www.lithoflex.org) and Tesseroids (http://tesseroids.leouieda.com/en/latest/, UIEDA *et alii*, 2011) for the calculations, which allows the flexural response calculations, the prism discretization of topography, and the gravity field calculations of both topography and mass changes at the Moho. In the calculations made by us the gravity field of the mass is calculated by discretization with prisms, and is more realistic than the flat Bouguer plate assumption. Height of calculation is 10 km, to be above all elevations. We use now standard values for the relevant parameters: crustal density 2,670 kg/m^3, mantle density 3,200 kg/m^3, reference depth for the Moho 35,000 m (BRAITENBERG *et alii*, 2003). The reference depth is the depth of the Moho in absence of elevation below or above the zero level. According to the measured GPS uplift rates, we impose an uplift of 2 mm/yr for the elevations above 4,000 m, and uplift of 0.7 mm/yr for elevations between 2,000 m and 4,000 m, and no uplift for lower elevation. The Moho is calculated first for today's topography in the isostatic local compensation model, to obtain a reference Moho against to which calculate the gravity change induced by the different uplift mechanisms, and then for the uplifted topography. In the first model, with unchanged crustal thickness, the uplift at Moho level is equal to the uplift of topography. For the second model Moho obeys the Airy isostatic response to topography uplift. We also test a mixed model, with a spatially varying mechanisms for a belt extending from the Himalayas to Tien Shan, as distinguished

from the Tibetan Plateau, with the aim of reproducing the observation of a positive gravity rate over Tibet and a negative rate south of the Tibetan Plateau. For the mixed model, we assume crustal thickening for the Himalayas-Tien Shan, and crustal uplift at the same rate as topography at Moho level for the Tibetan Plateau.

In Figure 3a the results for the gravity field changes are shown along profile AA' of Figure 1. The greatest positive change rate is found for the pure crustal uplift (first model: purple curve in central graph of Figure 3A), where mantle (yellow curve in top graph of Figure 3A) and elevated topography (red curve in top graph of Figure 3A) contribute a positive signal. Smallest change rate is found for the crustal thickening model (second, Airy isostatic model: green curve in central graph of Figure 3A), where the elevated mass surplus (red curve in top graph of Figure 3A) is cancelled out by the Moho deepening (blue curve in top graph of Figure 3A) leading to a gravity change close to zero. Assuming that the topography change is fully recovered from the GPS network, it is interesting to consider the signal generated at Moho level, as it implies different geodynamic models. It is seen that a pure crustal uplift can be distinguished from crustal thickening in the case of the Tibetan Plateau at the 10^{-8} $m/s^2/yr$ rate level. Figure 3b shows the expected field of the vertical gradient change rate, which would be the signal observed by a satellite mission as GOCE designed for picking up the time variable gradient change. The gradient picks up well the uplift of topography (red curve in top graph of Figure 3B) , but is not so sensitive in distinguishing a crustal thickening (green curve in mid graph of Figure 3B) from a pure crustal uplift (purple curve in mid graph of Figure 3B). The strongest gradient signal of elevation uplift is found where lateral elevation changes are strong.

The first and second models cannot reproduce a differential signal between Himalaya range and Himalaya foothill and the central Tibetan Plateau, as was observed from GRACE. We therefore modify the model assuming a differential crustal mechanism, with crustal thickening for the orogens

surrounding the Plateau from the Himalayas to the Tien Shan and lack of Moho deepening over the Tibetan Plateau. Equivalently it could be thought of phase transitions at the Moho level that densify the bottom crust. The result is shown in Figure 4. The uplift rate was kept equal as in the previous exercise, with the difference that over the Himalaya the crustal thickening is responding according to isostasy, whereas over Tibet crustal thickness is not changing and the entire crust is uplifting. Nearly the same results would be obtained by an uplifting topography and a stable depth of the Moho. The mixed model (green curve in mid graph of Figure 4A) is able to reproduce the higher positive gravity increase over the Tibetan Plateau, a lower positive increase over Himalaya, and a negative increase on the Indian Plate. This would correspond to the observations from GRACE (turqoise curve in mid graph of Figure 4A).

The change rate estimates consider the gravity effect, and reflect the signal observed by an airborne gravity survey. For terrestrial observations the decrease of gravity due to elevation change must be added to the calculated signal. In Figure 5 the gravity change rate for the two extreme models, the crustal thickening (Figure 5B) and the crustal uplift (Figure 5A) and for the mixed model (Tibetan Plateau crustal uplift, Himalayas-Tien Shan crustal thickening) (Figure 5C) is shown for the entire area and is compared to the observed residual GRACE rate (YI & SUN, 2014) (Figure 5D). The mixed model is closer to the observations than either one of the two end-member models.

Discussions

We first have shown that gravity change rates have been observed from terrestrial and satellite gravity observations over Tibet. The observed rates have an amplitude of a few μgal/year. The satellite derived rates have been compared to hydrological models and interpreted in terms of equivalent water layer variations, that is a mathematical model that projects the entire change rate signal into a surface water

layer of changing thickness. This equivalent water height is adequate for hydrologic purposes, as it is interpreted as water pumping from an aquifer or as glacier mass changes. When the signal is due to the combination of climatic and geodynamic effects, the equivalent water height model does not interpret the observed gravity signal correctly, as the sources are all placed at the Earth surface. We have tested different end-member situations concerning changes at Moho level in response to topographic level changes, and found that in the case of the Tibetan Plateau, the signal is of the same order of magnitude as the observed gravity change rates (Figure 3A).

Uncertainties on the uplift rate variations over the Plateau exist, but the existing observations from repeated leveling and GPS are consistent. Due to the EW striking homogeneity of the Plateau it can be assumed that also the western part of the Plateau is uplifting as the eastern part, probably with a NS variation. It may be argued that the crust is stratified and a full crustal model should be used for the simulations. Certainly a refined model can be done in the future, but the gross features and order of magnitude of the results will not change since the signal is governed by the greatest density contrasts, which are between land and air and between crust and mantle. The vertical shift of the crustal layers will only mildly contribute to the signal as only very small mass changes are involved with vertical movements inside the crust. Therefore the estimated gravity rates are realistic for the proposed model situation..

A future gravity mission with higher spatial resolution would allow to distinguish the subsiding Moho below the orogens placing tighter bounds on the geodynamic model. A higher spatial resolution compared to the present one of GRACE would allow to separate the climatic signal due to hydrology and ice from the tectonic signal which we show here to be present. An increased signal resolution combined with a higher spatial resolution would have the benefit of defining the geodynamic model better and then also the hydrologic estimate of drought in India, which can be expected to have a

smaller spatial scale than the tectonic signal. With the present resolution the two signals blend into a large scale positive or negative gravity variation.

Conclusions

This work describes a simulation of the expected gravity change rate over the Tibetan Plateau and surrounding orogens based on observed uplift rates of topography. The signal characteristics and amplitude have two extremes, corresponding to two end-member models. The maximum signal is reached for pure crustal uplift without crustal thickness change, the smallest signal is obtained for crustal thickening maintaining isostatic equilibrium where the topographic uplift is balanced by Moho lowering. We find that the crustal thickness signal cannot be neglected as it is within the order of magnitude of the expected hydrologic signal, the latter being generally used to interpret the gravity variation rates observed by GRACE satellites. For the Tibetan Plateau the observations give a positive gravity rate and a positive uplift rate, which is compatible with the crustal uplift model without crustal thickening. The positive gravity rate is not found for the Himalayas, although the range is presently uplifting, which is not compatible with the pure crustal uplift, but can be reproduced with the crustal thickening model. The distinction of the different mechanisms that lead to the topographic uplift is relevant in other disciplines, as in the modeling of crustal stresses and the estimate of accumulation of seismic energy. The simulations presented in this work give constraints for defining the requirements of the next generation of gravity satellite missions.

Acknowledgements

We thank Shuang Yi (Key Laboratory of Computational Geodynamics, University of Chinese Academy of Sciences, Beijing, China) for thoughtful comments. We thank Hans-Jürgen Götze (Christian Albrechts University Kiel), Cristiano Mendel Martins (Federal University Pará), Lavinia

Tunini (University of Barcelona) and one anonymous reviewer for excellent reviews. We acknowledge use of the mapping software GMT (WESSEL *et alii,* 2013).

References

AMANTE C. & EAKINS B.W. (2009) - *ETOPO1 1 Arc-Minute Global Relief Model: Procedures, Data Sources and Analysis*. NOAA Technical Memorandum NESDIS NGDC-24, 19 pp.

BRAITENBERG C., ZADRO M., FANG J., WANG Y., HSU H.T. (2000a). Gravity inversion in Quinghai-Tibet plateau, Physics and Chemistry of the Earth, **25,** 381-386.

BRAITENBERG C., ZADRO M., FANG J., WANG Y. & HSU, H.T. (2000b) - *The gravity and isostatic Moho undulations in Qinghai-Tibet plateau.* Journal of Geodynamics **30,** 489-505.

BRAITENBERG C., EBBING J. & GÖTZE, H.-J. (2002) - *Inverse modeling of elastic thickness by convolution method - The Eastern Alps as a case example.* Earth Planet. Sci. Lett., 202, 387-404.

BRAITENBERG C., WANG Y., FANG J. & HSU H.T. (2003) - *Spatial Variations of flexure parameters over the Tibet-Quinghai Plateau, Earth Planet.* Sci. Lett., **205**, 211-224.

BRAITENBERG C. (2014). *A grip on Geological Units with GOCE In: U. Marti (ed.), Gravity, Geoid and Height Systems,* International Association of Geodesy Symposia, **141**, 309-317, Springer, doi:10.1007/978-3-319-10837-7_39.

BRAITENBERG C. (2015) - *Exploration of tectonic structures with GOCE in Africa and across-continents.* Int. J.Appl. Earth Observ. Geoinf., **35**, 88-95. http://dx.doi.org/10.1016/j.jag.2014.01.013.

DECELLES P.G., ROBINSON D.M. & ZANDT G. (2002) - *Implications of shortening in the Himalayan foldthrust belt for uplift of the Tibetan Plateau.* Tectonics, **21**, 286–299. doi:10.1029/2001tc001322.

ERKAN K., SHUM C., WANG L., JEKELI C., LEE H., PANERO W., DUAN J., GUO J., HUANG Z. & WANG H. (2011) *Geodetic Constraints on the Qinghai-Tibetan Plateau Present-day Geophysical Processes.*Terr. Atmos. Ocean. Sci.*,* **22(2),** 141–253, doi: 10.3319/TAO.2010.09.27.01(TibXS).

FLOBERGHAGEN R., FEHRINGER M., LAMARRE D., MUZI D., FROMMKNECHT B., STEIGER C., PIÑEIRO J. & DA COSTA A. (2011) - *Mission design, operation and exploitation of the gravity field and steady-state ocean circulation explorer (GOCE) mission.* Journal of Geodesy **85**, 749-758.

GAN W., ZHANG P., SHEN Z.-K., NIU Z., WANG M., WAN Y., ZHOU D. & CHENG, J. (2007) - *Present-day crustal motion within the Tibetan Plateau inferred from GPS measurements.* Journal of Geophysical Research, **112**, B08416, DOI: 10.1029/2005JB004120

GOSCOMBE B. (2001) - *Tectonic map of the Himalayan Orogen*. Integrated Terrane Analysis Research (ITAR), Aldgate, 5154 South Australia, Unpublished Map.

HAO M., WANG Q., SHEN Z., CUI D., JI L. LI Y. & QIN S. (2014) - *Present day crustal vertical movement inferred from precise leveling data in eastern margin of Tibetan Plateau*. Tectonophysics, **632**, 281-292, http://dx.doi.org/10.1016/j.tecto.2014.06.016.

HOFMANN-WELLENHOF B. & MORITZ M. (2006) - Physical Geodesy, Springer Verlag, New York, ISBN 978-3-211-33544-4, 403 pp.

LAL D., HARRIS N.B.W., SHARMA K.K., GU Z., DING L., LIU T., DONG W., CAFFEE M.W. & JULL A.J.T. (2004) *Erosion history of the Tibetan Plateau since the last interglacial: Constraints from the first studies of cosmogenic 10Be from Tibetan bedrock,* Earth and Planetary Science Letters, **217,** 33-42. DOI: 10.1016/S0012-821X(03)00600-9

LI C., HILST R. VAN DER, MELTZER A. & ENGDAHL E. (2008) - *Subduction of the Indian lithosphere beneath the Tibet Plateau and Burma*. Earth Planet. Science Lett., **274**, 157-168.

LIANG S., GAN W., SHEN C., XIAO G., LIU J., CHEN W., DING X. & ZHOU D. (2013) - *Three-dimensional velocity field of present-day crustal motion of the Tibetan Plateau derived from GPS measurements.* Journal of Geophysical Research, **118**, 5722-5732. DOI: 10.1002/2013JB010503

MATSUO K. & HEKI K. (2010) - *Time-variable ice loss in Asian high mountains from satellite gravimetry,* Earth Planet. Sci. Lett., **290**, 30–36,doi:10.1016/j.epsl.2009.11.053.

MÉTIVIER F., GAUDEMER Y., TAPPONNIER P. & KLEIN M. (1999) *Mass accumulation rates in Asia during the Cenozoic,* Geophysical Journal International, **137**, 280-318. DOI: 10.1046/j.1365-246X.1999.00802.x.

PRIESTLEY K., JACKSON J. & MCKENZIE D. (2008) - *Lithospheric structure and deep earthquakes beneath India,the Himalaya and southern Tibet.* Geophys. J. Int., **172,** 345–362, doi: 10.1111/j.1365-246X.2007.03636.x.

RODELL M., HOUSER P.R., JAMBOR U., GOTTSCHALCK J., MITCHELL K., MENG C.-J., ARSENAULT K., COSGROVE B., RADAKOVICH J., BOSILOVICH M., ENTIN J.K., WALKER J.P., LOHMANN D. & TOLL, D.(2004) *The Global Land Data Assimilation System,* Bulletin of the American Meteorological Society, **85**, 381-394.

SAMPIETRO D., REGUZZONI M. & BRAITENBERG C. (2014). *THE GOCE ESTIMATED MOHO BENEATH THE TIBETAN PLATEAU AND HIMALAYA. In*: *C. RIZOS, P. WILLIS (EDS.), Earth on the Edge: Science for a Sustainable Planet*, International Association of Geodesy Symposia, **139**, Springer, 391-397, doi:10.1007/978-3-642-37222-3_52.

SATO T., MIURA S., SUN W., SUGANO T., FREYMUELLER J.T., LARSEN C.F., OHTA Y., FUJIMOTO H., INAZU D. & MOTYKA R. J. (2012) - *Gravity and uplift rates observed in southeast Alaska and their comparison with GIA model predictions*, J. Geophys. Res., **117**, B01401, doi:10.1029/2011JB008485.

SCHÖN J.H. (2011) – *Physical properties of Rocks, A Workbook,* Handbook of Petroleum Exploration and Production, **8**, Elsevier,1-481, ISBN: 978-0-444-53796-6.

SHIN Y. H., XU X., BRAITENBERG C., FANG J. & WANG, Y. (2007) - *Moho undulations beneath Tibet from GRACE-integrated gravity data*. Geophys. J. Int., doi: 10.1111/j.1365-246X.2007.03457.x, 1-15.

SHIN Y. H., SHUM, C. K., BRAITENBERG C., LEE S. M., XU H., CHOI K. S., J. H. BAEK & PARK J. U. (2009). *Three-dimensional fold structure of the Tibetan Moho from GRACE gravity data,* Geophysical Research Letters, **36**,L01302, doi:10.1029/2008GL036068.

SHIN Y.H., SHUM C.K., BRAITENBERG C., LEE S.M., NA S.-H., SUN K.C., HSU H., PARK Y.-S, LIM M. (2015) - *Moho topography, ranges and folds of Tibet by analysis of global gravity models and GOCE data*, Scientific Reports, Nature Publishing Group, **5: 11681**, doi: 10.1038/SREP11681, 1-7.

SUN W., WANG Q., LI H., WANG Y., OKUBO S., SHAO D., LIU D. & FU G. (2009) - *Gravity and GPS measurements reveal mass loss beneath the Tibetan Plateau: Geodetic evidence of increasing crustal thickness,* Geophys. Res. Lett., **36**, L02303,doi:10.1029/2008GL036512.

TAPLEY B.D., BETTADPUR S., RIES J., THOMPSON P. & WATKINS M. (2004) - *GRACE measurements of mass variability in the Earth system*. Science, **305**, 503-505.

TIMMEN L., GITLEIN O., MÜLLER J., STRYKOWSKI G. & FORSBERG R (2008) - *Absolute gravimetry with the Hannover meters JILAg-3 and FG5-220, and their deployment in a Danish-German cooperation*, Zeitschrift für Vermessungswesen, **3/2008**, 149-163.

TIMMEN L., GITLEIN O., MÜLLER J., DENKER H., MÄKINEN J., BILKER M., PETTERSEN B. R., LYSAKER D. I., OMANG O. C. D., SVENDSEN J. G. G., WILMES H., FALK R., REINHOLD A., HOPPE W., SCHERNECK H.-G., ENGEN B., HARSSON B. G., ENGFELDT A., LILJE M., STRYKOWSKI G. & FORSBERG R. (2006) - Observing Fennoscandian Gravity Change by Absolute Gravimetry. In: F. SANSÒ, A. J. GIL (EDS.): *Geodetic Deformation Monitoring: From Geophysical to Engineering Roles*, International Association of Geodesy Symposia, 131, Springer, 193–199.

TORGE W. (1991) *The present state of absolute gravimetry.* In: Cahiers du Centre Europeen de Geodynamique et de Seismologie. 3, 9–22, Luxembourg.

TORGE W. (2001) *Geodesy*, third edition, ISBN 3-11-017072-8, De Gruyter, Berlin, 1-416.

UIEDA L., BOMFIM E. P., BRAITENBERG C.& MOLINA E. (2011) - *Optimal forward calculation method of the Marussi tensor due to a geologic structure at GOCE height*, 75. Proc. of '4th International GOCE User Workshop', Munich, Germany, 31 March - 1 April 2011 (ESA SP-696, July 2011),

WANG Q., ZHANG P.-Z., FREYMUELLER J.T., BILHAM R., LARSON K.M., LAI X., YOU X., NIU Z., WU J., LI Y., LIU J., YANG Z. & CHEN Q. (2001) - *Present-day crustal deformation in China constrained by global positioning system measurements*. Science, **294** (5542), 574-577. DOI: 10.1126/science.1063647.

WANG C. Y., HAN W. B., WU J. P., LOU H. & CHAN W. W. (2007) - *Crustal structure beneath the eastern margin of the Tibetan Plateau and its tectonic implications.* Journal of Geophysical Research: Solid Earth, **112**, 1978–2012.

WESSEL P., SMITH W. H. F., SCHARROO R., LUIS J. F. & WOBBE F. (2013) *Generic Mapping Tools: Improved version released,* EOS Trans. AGU, **94**, 409-410.

YI S., & SUN W. (2014) - *Evaluation of glacier changes in high-mountain Asia based on 10 year GRACE RL05 models*, J. Geophys. Res. Solid Earth, **119**, doi:10.1002/2013JB010860.

YIN A., & HARRISON T.M. (2000) *Geologic Evolution of the Himalayan-Tibetan orogen*, Annu. Rev. Earth Planet. Sci., **28**, 211–280.**Figure captions**

Figure 1- Topography of Tibet Plateau including the Himalayas. Rivers and Coastlines in Blue. National borders in thin black. Principal faults and geologic boundaries in heavy black. AA' is the profile along which gravity is calculated and shown in Figures 3 and 4. MBT: Main Boundary Thrust. ITS: Indus Tsangpo Suture. BNS: Bangong Nujian Suture. JS: Jinsha Sutrue, ATF: Altyn Tagh Fault. Triangles: Absolute gravity stations discussed in text. Pink outline: High Himalayas. Green Outline: Lesser Himalayas. Adopted from (YIN & HARRISON, 2000) and GOSCOMBE (2001).

Figure 2 – Schematic illustrating the geodynamic models of crustal thickening and crustal uplift and the corresponding mass changes. A Crustal uplift without thickness change. B Crustal thickening model. C Mixed model, with crustal uplift over the Plateau and crustal thickening for the Himalayas. Yellow: positive mass change at topography; red: positive mass change at Moho level; blue: negative mass change at Moho level.

Figure 3 Gravity changes over the Tibetan Plateau including the Himalayas for two different geodynamic models. Elevation increases at the rate of 2 mm/yr, accompanied with crustal thickening or with constant crustal thickness, which is uplifting. A) Gravity field B) Vertical Gravity Gradient. Location of profile shown in Figure 1 as AA'; the origin of the profile is in point A, the end in point A'.

Figure 4- Gravity changes over the Tibetan Plateau and the Himalayas for a mixed geodynamic model in the Tibetan Plateau and the Himalayas. Elevation increases at the rate of 2 mm/yr, accompanied with crustal thickening in the Himalayas and with constant crustal thickness, which is uplifting in the Tibetan Plateau. A) Gravity field. B) Gradient field. Location of profile shown in Figure 1 as AA'; the origin of the profile is in point A, the end in point A'.

Figure 5- Gravity response of different geodynamic models for a given topographic uplift over Tibet and Himalaya and observed gravity rate. Elevation increases at the rate of 2 mm/yr, accompanied with A) crustal uplift everywhere B) crustal thickening everywhere C) mixed model, with crustal thickening from Himalaya to Tien Shan and with constant crustal thickness which is uplifting in Tibet. White outline gives the area in which crustal thickening is assigned. D) Residual gravity rate from satellite GRACE according to YI & SUN (2014). Blue lines: rivers;

Table captions

Table 1- Gravity change rates mentioned in the text.

Table 2- Expected and observed ratios between gravity and station height rates mentioned in the text.

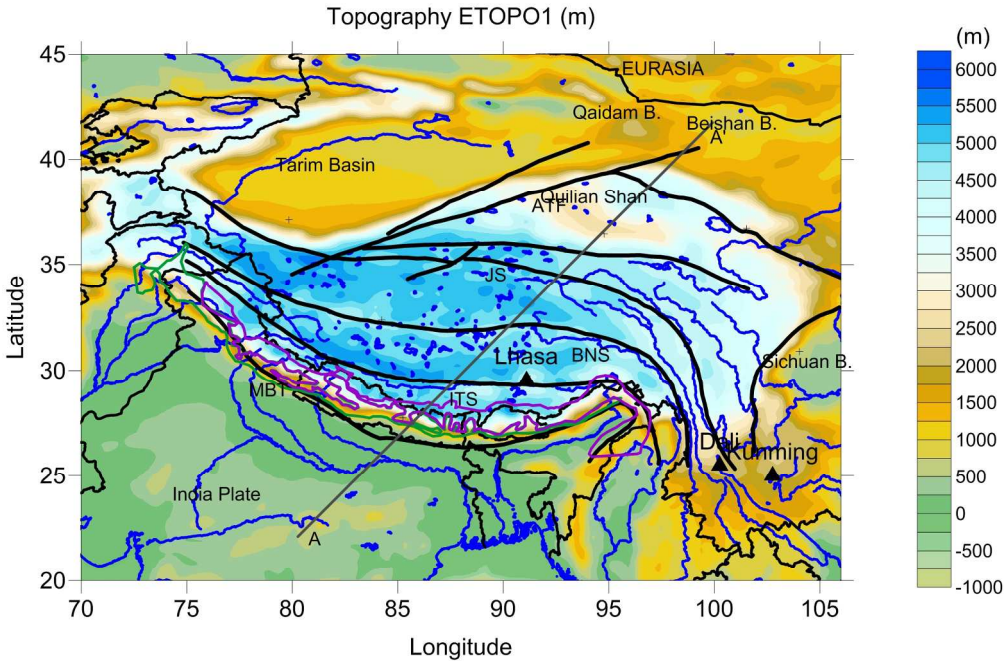

Figure 1- Topography of Tibet Plateau including the Himalayas. Rivers and Coastlines in Blue. National borders in thin black. Principal faults and geologic boundaries in heavy black. AA' is the profile along which gravity is calculated and shown in Figures 3 and 4. MBT: Main Boundary Thrust. ITS: Indus Tsangpo Suture. BNS: Bangong Nujian Suture. JS: Jinsha Sutrue, ATF: Altyn Tagh Fault. Triangles: Absolute gravity stations discussed in text. Pink outline: High Himalayas. Green Outline: Lesser Himalayas. Adopted from (YIN & HARRISON, 2000) and GOSCOMBE (2001).
189x124mm (299 x 299 DPI)

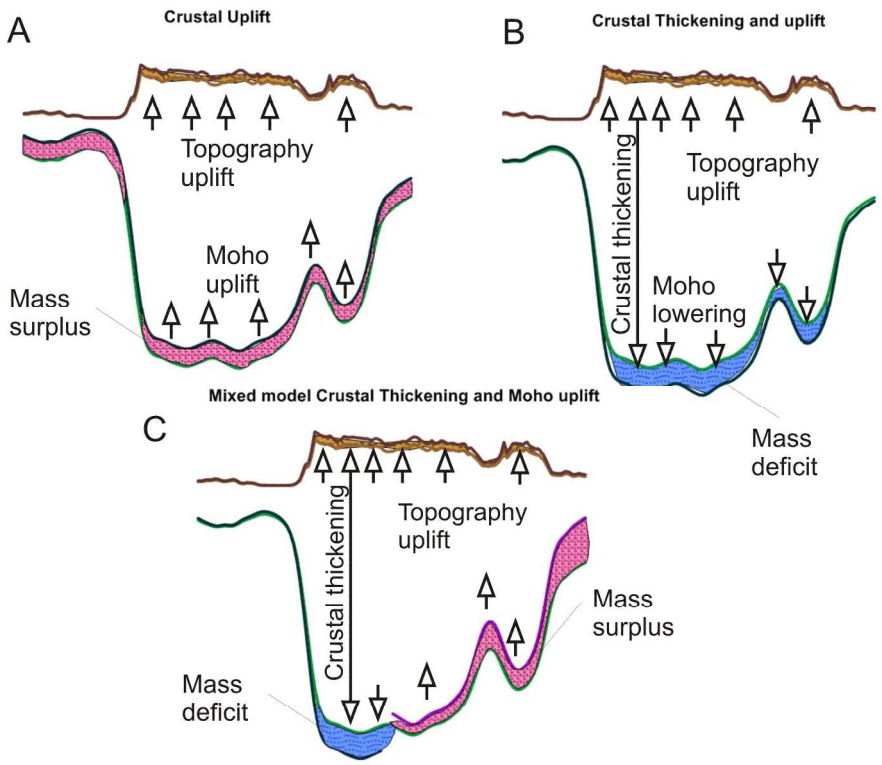

Figure 2 – Schematic illustrating the geodynamic models of crustal thickening and crustal uplift and the corresponding mass changes. A Crustal uplift without thickness change. B Crustal thickening model. C Mixed model, with crustal uplift over the Plateau and crustal thickening for the Himalayas. Yellow: positive mass change at topography; red: positive mass change at Moho level; blue: negative mass change at Moho level.
241x192mm (300 x 300 DPI)

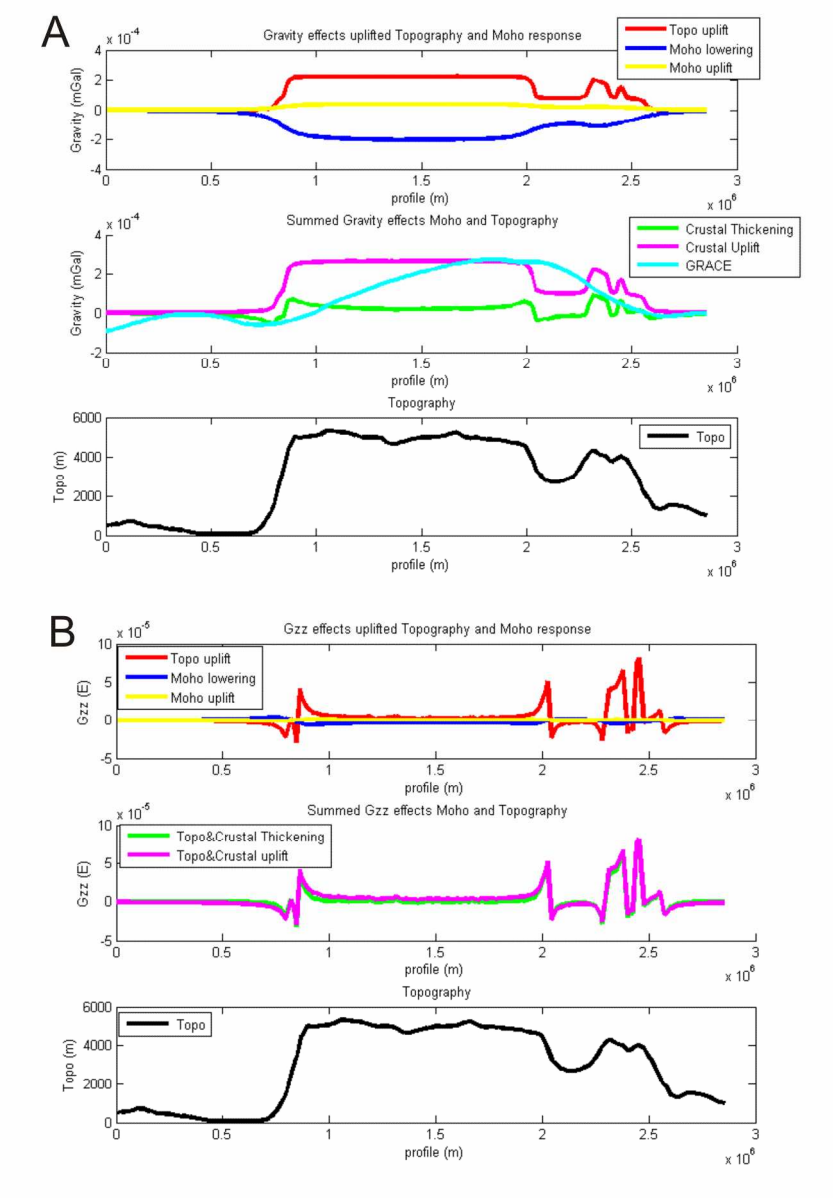

Figure 3 Gravity changes over the Tibetan Plateau including the Himalayas for two different geodynamic models. Elevation increases at the rate of 2 mm/yr, accompanied with crustal thickening or with constant crustal thickness, which is uplifting. A) Gravity field B) Vertical Gravity Gradient. Location of profile shown in Figure 1 as AA'; the origin of the profile is in point A, the end in point A'.

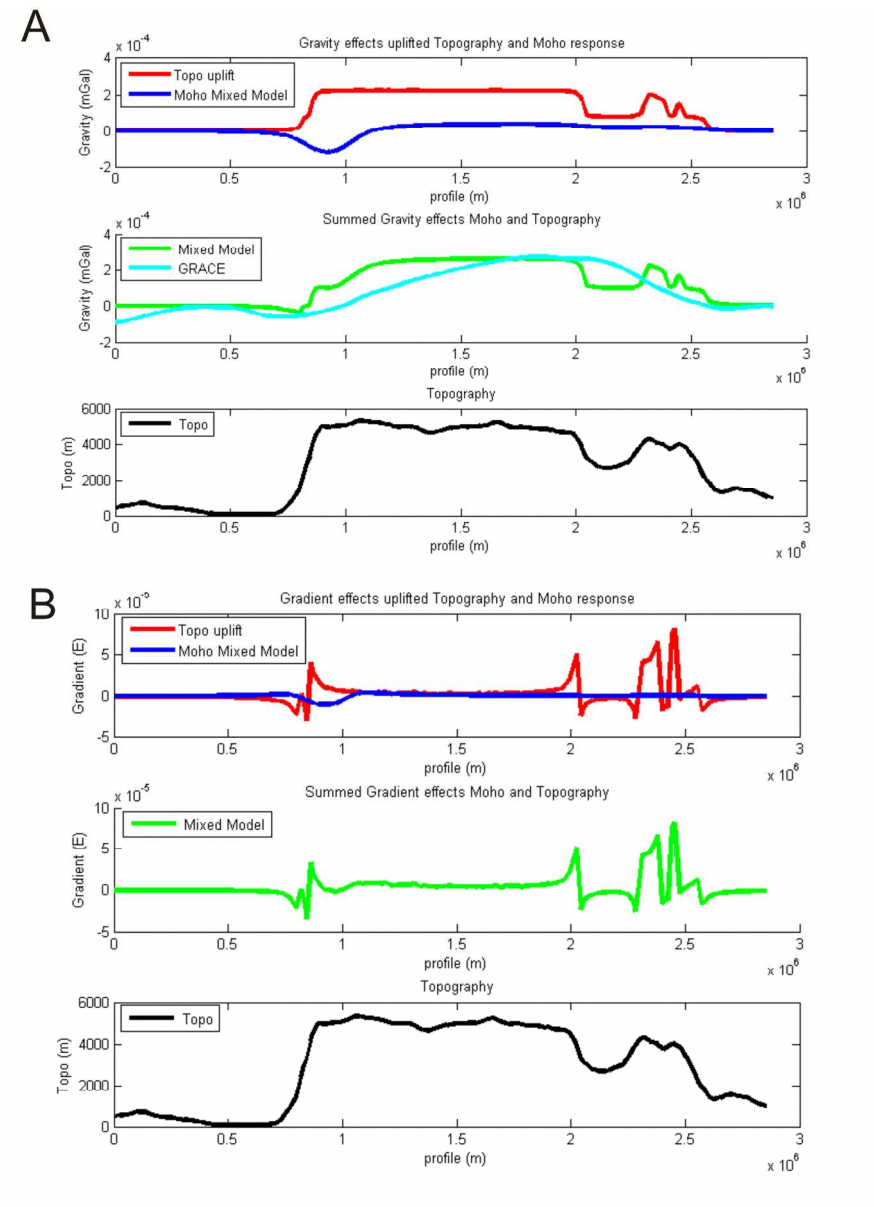

Figure 4- Gravity changes over the Tibetan Plateau and the Himalayas for a mixed geodynamic model in the Tibetan Plateau and the Himalayas. Elevation increases at the rate of 2 mm/yr, accompanied with crustal thickening in the Himalayas and with constant crustal thickness, which is uplifting in the Tibetan Plateau. A) Gravity field. B) Gradient field. Location of profile shown in Figure 1 as AA'; the origin of the profile is in point A, the end in point A'.

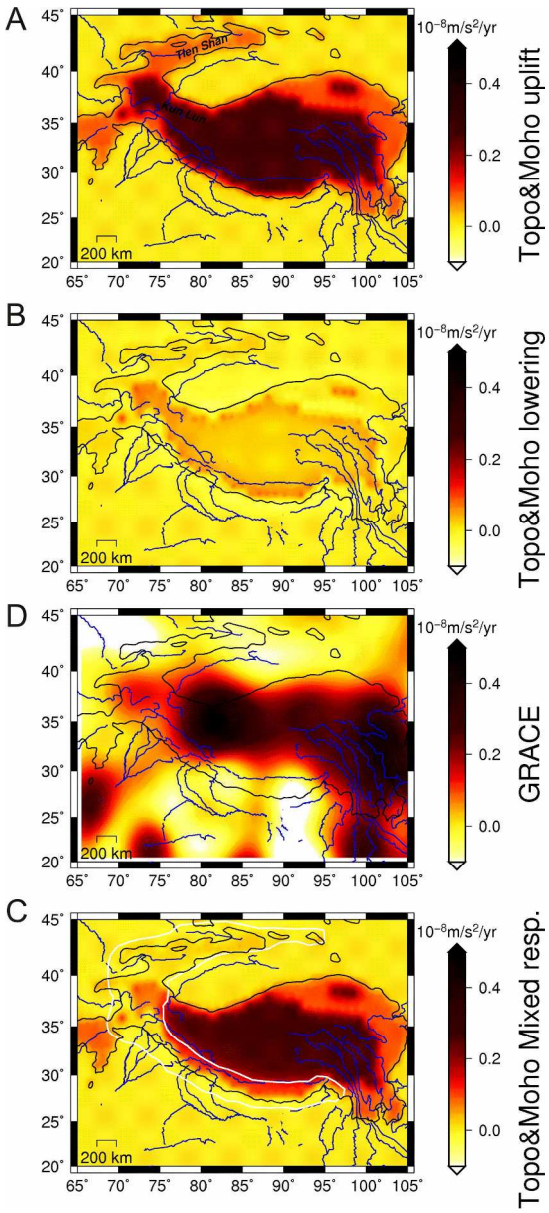

Figure 5- Gravity response of different geodynamic models for a given topographic uplift over Tibet and Himalaya and observed gravity rate. Elevation increases at the rate of 2 mm/yr, accompanied with A) crustal uplift everywhere B) crustal thickening everywhere C) mixed model, with crustal thickening from Himalaya to Tien Shan and with constant crustal thickness which is uplifting in Tibet. White outline gives the area in which crustal thickening is assigned. D) Residual gravity rate from satellite GRACE according to YI & SUN (2014). Blue lines: rivers;

Table 1

Station	method	Gravity rate	Height rate	Gravity rate corrected for denudation and uplift	Author
Lhasa	Absolute gravity observation	-1.97±0.66 10^{-8} m/s^2/yr	+0.8±0.5 mm/yr	-1.56±0.67 10^{-8} m/s^2/yr	SUN *et alii* (2009)
Kunming	Absolute gravity observation	-1.42±0.38 10^{-8} m/s^2/yr	+2.3±0.5 mm/yr	-0.73±0.39 10^{-8} m/s^2/yr	SUN *et alii* (2009)
Dali	Absolute gravity observation	-0.41±0.24 10^{-8} m/s^2/yr	+0.5±0.5 mm/yr	-0.06±0.26 10^{-8} m/s^2/yr	SUN *et alii* (2009)
Gravity change at station due to uplift	Flat Bouguer estimate+vertical gravity gradient	-0.19 10^{-8} m/s^2/mm	----------	----------	SUN *et alii* (2009)
Erosional denudation over Tibet plateau	estimated	-0.25±0.1 10^{-8} m/s^2/yr	----------	----------	SUN *et alii* (2009)
Moho lowering	estimated	-0.78 10^{-8} m/s^2/yr	2.3 cm/yr	----------	SUN *et alii* (2009)

Table 2

Station or model situation	Ratio: gravity/uplift	Model parameters
Topography uplift, no mass change at Moho level	-0.19 10^{-8} m/s^2/mm	$\rho_c = 2{,}670$ kg/m^3 $\rho_m = 3{,}200$ kg/m^3
Topography and Moho uplift	-0.17 10^{-8} m/s^2/mm	"
Lhasa	-2.4 10^{-8} m/s^2/mm	Gravity and uplift rates from SUN *et alii* (2009)
Kunming	-0.6 10^{-8} m/s^2/mm	"
Dali	-0.8 10^{-8} m/s^2/mm	"